Published in final edited form as:
Mol Cancer Ther. 2013 November ; 12(11): . doi:10.1158/1535-7163.MCT-13-0040.

UNC569, a novel small molecule Mer inhibitor with efficacy against acute lymphoblastic leukemia *in vitro* and *in vivo*

Sandra Christoph[1,2], **Deborah DeRyckere**[1], **Jennifer Schlegel**[1], **J. Kimble Frazer**[3], **Lance A. Batchelor**[3], **Alesia Y. Trakhimets**[4], **Susan Sather**[1], **Debra M. Hunter**[7], **Christopher Cummings**[1], **Jing Liu**[5], **Chao Yang**[5], **Dmitri Kireev**[5], **Catherine Simpson**[5], **Jacqueline Norris-Drouin**[5], **Emily A. Hull-Ryde**[5], **William P. Janzen**[5,6], **Gary L. Johnson**[6,7], **Xiaodong Wang**[5], **Stephen V. Frye**[5,7], **H. Shelton Earp III**[6,7], and **Douglas K. Graham**[1]

[1]Department of Pediatrics, University of Colorado Anschutz Medical Campus, Aurora, CO, USA

[2]Department of Bone Marrow Transplantation, University Hospital Essen, Essen, Germany

[3]Section of Pediatric Hematology/Oncology, University of Oklahoma Health Sciences Center, Oklahoma City, OK, USA

[4]Undergraduate Research Opportunities Program, University of Utah, Salt Lake City, UT, USA

[5]Center for Integrative Chemical Biology and Drug Discovery, Division of Chemical Biology and Medicinal Chemistry, Eshelman School of Pharmacy, University of North Carolina at Chapel Hill, Chapel Hill, NC, USA

[6]Department of Pharmacology, University of North Carolina at Chapel Hill, Chapel Hill, NC, USA

[7]Lineberger Comprehensive Cancer Center, Department of Medicine, School of Medicine, University of North Carolina at Chapel Hill, Chapel Hill, NC, USA

Abstract

Acute lymphoblastic leukemia (ALL) is the most common malignancy in children. Although survival rates have improved, patients with certain biological subtypes still have suboptimal outcomes. Current chemotherapeutic regimens are associated with short- and long-term toxicities and novel, less toxic therapeutic strategies are needed. Mer receptor tyrosine kinase is ectopically expressed in ALL patient samples and cell lines. Inhibition of Mer expression reduces pro-survival signaling, increases chemosensitivity, and delays development of leukaemia *in vivo* suggesting that Mer tyrosine kinase inhibitors are excellent candidates for targeted therapies. Brain and spinal tumors are the second most common malignancies in childhood. Multiple chemotherapy approaches and radiation have been attempted, yet overall survival remains dismal. Mer is also abnormally expressed in atypical teratoid/rhabdoid tumors (ATRT), providing a rationale for targeting Mer as a therapeutic strategy. We have previously described UNC569, the first small molecule Mer inhibitor. This manuscript describes the biochemical and biological effects of UNC569 in ALL and ATRT. UNC569 inhibited Mer activation and downstream signaling through ERK1/2 and AKT, determined by western blot analysis. Treatment with UNC569 reduced proliferation/survival in liquid culture, decreased colony formation in methylcellulose/soft agar, and increased sensitivity to cytotoxic chemotherapies. *MYC* transgenic zebrafish with T-ALL were treated with UNC569 (4 μM for 2 weeks). Fluorescence was quantified as indicator of the distribution of lymphoblasts, which express Mer and enhanced green fluorescent protein. UNC569

Corresponding authors: Douglas K. Graham, Department of Pediatrics, University of Colorado Anschutz Medical Campus, Mail Stop 8302, PO Box 6511, Aurora, CO 80045, USA; Phone: (303) 724-4006; Fax: 303-724-4015; doug.graham@ucdenver.edu.

Conflicts of interest: Wang, X.; Liu, J.; Yang, C.; Zhang, W.; Frye, S.V.; Kireev, D. Pyrazolopyrimidine Compounds for the Treatment of Cancer. WO Patent 2011146313, 2011.

induced >50% reduction in tumor burden compared to vehicle- and mock-treated fish. These data support further development of Mer inhibitors as effective therapies in ALL and ATRT.

Keywords

UNC569; Mer Inhibitor; Treatment of ALL

Introduction

Acute lymphoblastic leukemia (ALL) is the most common malignancy in children and represents nearly 30% of all pediatric cancers (1;2). Although the overall survival rate for pediatric B-cell ALL is approximately 85%, specific biological subtypes, including T-ALL, have a poorer prognosis even with current therapeutic protocols and treatment of relapsed ALL remains a challenge (3). In addition, the intensified therapy used in current protocols is associated with a significant and increased risk for short- and long-term toxicities (slowed growth, organ damage, and secondary malignancy) (4;5). Therefore, novel, more effective, and less toxic therapies are needed.

Tyrosine kinases are frequently abnormally regulated in cancer cells. Overexpression of Mer receptor tyrosine kinase, a member of the TAM (Tyro3/Axl/Mer) family of receptor tyrosine kinases, has been reported in a variety of human cancers, including B- and T- ALL (6–8). Ectopic expression of Mer in lymphocytes in transgenic mice promotes the development of leukemia/lymphoma (9;10). In humans, Mer is ectopically expressed in pediatric T-cell ALL and pre-B-cell ALL patient samples. In contrast, Mer is not expressed in normal mouse and human T- and B-lymphocytes at any stage of development (11). Inhibition of Mer expression by shRNA has been shown to reduce pro-survival signaling, dramatically increase the sensitivity of leukemia cells to cytotoxic agents, and significantly delay development of leukemia in a mouse model (12;13). Taken together, these data provide a rationale for targeting Mer as a therapeutic strategy in ALL.

Brain and spinal tumors are the second most common malignancies in childhood after leukemia (14). Atypical teratoid rhabdoid tumors (ATRTs) are rare tumors of the central nervous system. However, in patients less than 3 years of age this tumor accounts for up to 20% of cases. Multiple chemotherapy approaches and radiation have been attempted, yet overall survival remains dismal (15). This aggressive tumor remains a significant challenge in pediatric neuro-oncology, and new therapeutic approaches are needed. The abnormal expression of Mer in ATRT cells provides a rationale for targeting Mer as a therapeutic strategy in this aggressive cancer type.

In the past several years, tyrosine kinase inhibitors (TKI) have taken on an increasingly important role in the treatment of cancer. Imatinib, a selective inhibitor of the BCR-ABL tyrosine kinase most impressively validated the concept of designing a small molecule TKI to treat a defined patient population. The improvement in survival has been dramatic in chronic myeloid leukaemia, which is driven by the BCR-ABL translocation (16). Because some patients experienced relapse due to resistance-conferring point mutations within BCR-ABL, the second-generation ABL kinase inhibitors nilotinib and dasatinib were developed and other ABL kinase inhibitors with activity against BCR-ABL (T315I) including ponatinib are being investigated (17;18). Other examples of small molecule TKI under investigation are vandetanib in the management of medullary thyroid cancer (19), lapatinib for the treatment of hormone-positive and HER2-positive advanced breast cancer (20), erlotinib and gefitinib for elderly patients with advanced non-small-cell lung cancer (21), sunitinib for the treatment of metastatic renal cell carcinoma (22), sorafenib against acute

myeloid leukemia (23) and vemurafenib against melanoma with BRAF V600E mutation (24).

Targeted therapy aimed at a specific cancer-promoting signaling pathway is expected to allow for a more efficacious clinical response in patients with ALL and significantly reduce toxicities. Recent successes in the treatment of cancer with small molecule TKI has encouraged us to develop a small molecule Mer tyrosine kinase inhibitor (Mer TKI) as a selective therapeutic for ALL (25;26). We have previously reported the first in class Mer-selective small molecule inhibitor UNC569 (27). UNC569 (Figure 1) is a pyrazolopyrimidine with potent activity against Mer (Mer IC_{50} = 2.9 nM, Axl IC_{50}=37 nM, Tyro3 IC_{50} = 48 nM). The studies described here demonstrate anti-oncogenic properties mediated by UNC569 in ALL cell lines, in a transgenic zebrafish T-ALL model and in atypical teratoid rhabdoid tumors.

Materials and Methods

Tissue culture

Jurkat (T-ALL) and 697 (B-ALL) human leukemia cell lines were obtained from the American Type Culture Collection, ATCC (Manassas, VA) and from the German Collection of Microorganisms and Cell Cultures, DSMZ (Braunschweig, Germany). These cell lines were cultured in RPMI-1640 media (Hyclone Laboratories, Logan, UT) supplemented with 10% fetal bovine serum (FBS) (Atlanta Biologicals, Lawrenceville, GA) and penicillin/streptomycin (100 units/ml and 100 μg/ml, Hyclone Laboratories, Logan, UT). The atypical teratoid rhabdoid tumor cell line, BT12 were obtained from Bernard Weissman (UNC Lineberger) and were grown in RPMI-1640 media supplemented with 15% fetal bovine serum and penicillin/streptomycin (100 units/ml and 100 μg/ml). Cells were maintained at 37°C in a humidified atmosphere containing 5% CO_2. The 697 and the Jurkat cell lines were authenticated. The identities of 697 (6/2012) and Jurkat (12/2012) cell lines were confirmed by short tandem repeat analysis (28) and matched with the information in the DSMZ database. At this time there is no STR profile publicly available for the BT12 cell line. However the STR profiles (12/2012) are singular and do not match any in the ATCC or DSMZ collections. All cell cultures were tested negative for mycoplasma contamination. Recombinant human growth arrest-specific protein 6 (Gas6) (#885-GS, R&D Systems, Minneapolis, MN) was reconstituted in PBS. Inhibitor UNC569 was synthesized as previously described (27) and stock solutions were prepared in DMSO at 3 mM.

Immunoprecipitation and detection of phosphorylated Mer

ALL cell cultures were treated with 0.12 mM pervanadate for 3 minutes to stabilize the phosphorylated form of Mer. Cells were lysed in 50 mM HEPES (pH 7.5), 150 mM NaCl, 10 mM EDTA, 10% (v/v) glycerol, 1% (v/v) Triton X-100, 1 mM sodium orthovanadate, 0.1 mM sodium molybdate, and protease inhibitors (Complete mini, Roche Molecular Biochemicals, Indianapolis, IN) and Mer was immunoprecipitated by incubating with mouse monoclonal anti-Mer antibody (MAB8912, R&D Systems, Minneapolis, MN) and rec-Protein G-sepharose 4B beads (#10-1242, Invitrogen, Grand Island, NY). Immune complexes were collected by centrifugation and washed with lysis buffer. Beads were resuspended in Laemmli buffer (62.5 mM Tri-HCl pH 6.8, 25% glycerol, 5% β-mercaptoethanol, 2% SDS, and 0.01% bromophenol blue) and boiled to elute bound protein. Phosphorylated and total Mer proteins were detected by western blot using a proprietary α-phospho Mer antibody (29) (PhosphoSolutions, Aurora, CO) and anti-human Mer antibody (#1633-1, Epitomics, Burlingame, CA). To determine the relative changes in phosphorylation between UNC569-treated and untreated cells, the densities of individual bands were measured using ImageJ software (National Institute of Health). IC_{50} values were

determined by non-linear regression using GraphPad Prism software (v5.0, GraphPad Software, LaJolla, CA). BT12 cells were pre-incubated with the indicated UNC569 concentration followed by treatment with pervanadate as above. Cells were lysed, immunoprecipitated with polyclonal C-terminal Mer antibody N-14 (30) and subjected to SDS-polyacrylamide gel electrophoresis.

Western blot analysis

Whole cell lysates were prepared and resolved by SDS-PAGE. The following antibodies from Cell Signaling Technology (Danvers, MA) were used for western blot analysis according to manufacturer recommendations: anti-phospho-Akt (Ser473, #9271), anti-Akt (#9272); anti-phospho-p44/42 MAPK (pErk1/2, Thr202/Tyr204, #9106), anti-p44/42 MAPK (Erk1/2, #9102), anti-PARP (#9542), anti-Caspase 3 (#9662), anti-Tubulin (#2125), anti-Tyro3 (#5585) and anti-GAPDH (#3683, HRP). Anti-Actin antibody (#sc-1616 HRP) was purchased from Santa Cruz Biotechnology (Santa Cruz, CA) and Anti-Axl antibody (#AF154) was purchased from R&D Systems. Primary antibodies were labeled with HRP-conjugated secondary antibodies (donkey-anti-goat, #sc-2020, Santa Cruz Biotechnology; goat-anti-mouse, #170-6516, Bio-Rad Laboratories, Hercules, CA; or donkey-anti-rabbit, #711-035-152, Jackson ImmunoResearch Laboratories, West Grove, PA) and proteins were visualized by enhanced chemiluminescence (Perkin-Elmer, Waltham, MA). For BT12 experiments gels with electrophoresed, Mer immunoprecipitates were transferred and blotted with phosphotyrosine antibody (#sc-508 HRP) or back blotted with the NIH anti-Mer polyclonal.

Colorimetric assay for detection of metabolically active cells

Jurkat and 697 cells were plated at optimal density in 96-well plates (3×10^5 cells/ml) and cultured for 8 hours before addition of UNC569 or an equivalent volume of DMSO control. After 24 hours cells were harvested and plated in fresh medium containing UNC569 or vehicle only for an additional 24 hours. MTT reagent (3-(4,5-Dimethyl-2-thiazolyl)-2,5-diphenyl-2H-tetrazolium bromide, #M5655 Sigma, St. Louis, MO) was added to a final concentration of 0.65 mg/ml and the cells were incubated for another 4 hours. Solubilization solution (2×, 10% sodium duodecyl sulfate in 0.01 M HCl) was added and plates were incubated at 37°C overnight. Optical density was determined at 562 nm with a reference wavelength of 650 nm. BT12 cells were plated at optimal density in 96 well plates (5×10^3 cells/ml) and cultured for 8 hours before addition of UNC569 or an equivalent volume of DMSO control. After 48 hours, 20 μl of MTS (3-(4,5-dimethyl-2-yl)-5-(3-carboxymethoxyphenyl)-2-(4-sulfophenyl)-2H-tetrazolium) reagent (Cell Titer 96 Aqueous One Solution Reagent #G3582, Promega, Madison, WI) was added to each well. The cells were incubated for 4 hours. Absorbance was recorded at 490 nm using a 96-well plate reader. Relative cell numbers for all cell lines were calculated by subtraction of background absorbance and normalization to untreated controls. IC_{50}-values were determined by nonlinear regression using GraphPad Prism software.

Apoptosis assay

Jurkat or 697 cells were plated at 3×10^5 cells/ml and treated with UNC569 and/or cytotoxic agents (methotrexate, #A6770, Sigma, St. Louis, MO; etoposide, #341205, CalBiochem, Billerica, MA) for 48 hours. Alternatively, cells were treated with UNC569 for 24 hours, then harvested and cultured in fresh medium containing UNC569 or vehicle only for an additional 24 hours. Cells were collected by centrifugation at 240g for 5 minutes. Cell pellets were resuspended in PBS containing 1 μM YO-PRO-1 (Y3603, Invitrogen, Grand Island, NY) and 1.5 μM propidium iodide (P3566, Invitrogen). Samples were incubated for 15 minutes and fluorescence was detected using a FC500 flow cytometer and analyzed with CXP data analysis software (Beckman Coulter, Krefeld, Germany).

Methylcellulose assay

Jurkat or 697 cells were plated in methylcellulose-based medium (#1101, ReachBio, Seattle, WA) containing UNC569 or DMSO control according to manufacturer's protocol (500 cells/ml methylcellulose, 35 mm plates). After the initial plating, additional UNC569 or DMSO control was added to the top of the methylcellulose in a volume of 100 μl every other day. Colonies were grown for eight days and then counted. Bright field images were taken with a spinning disk confocal 3I Marianas (Intelligent Imaging Innovations Inc., Denver, CO) based on a inverted Zeiss Axio Observer Z1 (Carl Zeiss Inc., Jenna, Germany). A CoolSnap HQ2 camera featuring 1392 × 1040 imaging pixels (Photometrics Inc., Tucson, AZ) via a 5× Zeiss air objective was used. As imaging acquisition software Slidebook 5.0 (Intelligent Imaging Innovations, Inc., Denver, CO) was utilized. Single colony pictures were generated using a Nikon Eclipse TS100 microscope (Nikon Inc., Melville, NY) with Nikon Plan 10X, numerical aperture 0.25 objective lens and with a Nikon Digital Sight DS-L2 camera equipped with Firmware DS-L2 Ver4.60.

Soft agar assay

BT12 cells were plated in 0.7% agarose (#CA3510-8 Denville Scientific, South Plainfield, NJ) over a higher percentage agar base layer. Agarose was overlaid with medium (RPMI-1640 media supplemented with 15% fetal bovine serum and penicillin/streptomycin (100 units/ml and 100 μg/ml)) with UNC569. Medium and UNC569 were renewed twice weekly. Colonies were grown for 14 days prior to staining with 2 mg/ml MTT (#M5655, Sigma). Representative pictures are scans made with Perfection V700 Scanner (Epson, Long Beach, CA) and subsequent counting using ImageJ Software.

Leukemic zebrafish experiments

Transgenic zebrafish expressing human MYC in lymphocytes (31) were crossed to *lck::EGFP* zebrafish (32). Leukemic fish were identified via fluorescence microscopy and images were captured using an Olympus MVX10 Microscope with a SPOT Insight Camera and software package. Zebrafish with cancer were then treated by "immersion assay," as described previously (33). Briefly, fish were housed in 4 μM UNC569 plus DMSO, equimolar DMSO vehicle alone, or water only. Daily water changes with fresh drug were performed for a treatment duration of 14 days. Fluorescent images were captured at day 14 for comparison to pre-treatment images. Images were normalized to an internal reference standard. Fluorescence intensity was determined using ImageJ software and plotted as a three-dimensional spatial representation for each image. Plots were integrated to generate volumetric quantifications of the area under the curve. GFP fluorescence was compared in the same fish pre- and post-treatment to assess responses, reflected as per cent gain or loss in GFP intensity (termed the "GFP score").

Statistical analyses

Statistically significant differences between means were determined using a two-tailed, unpaired Student's t-tests for zebrafish and cell culture experiments, respectively. The level of significance for all statistical analyses was chosen a priori to be $p < 0.05$. Statistical analyses were carried out using GraphPad Prism software (Version 5.0, GraphPad Software, LaJolla, CA).

Results

UNC569 inhibits Mer and downstream oncogenic signaling pathways in ALL cells

Activation of Mer stimulates proliferative and anti-apoptotic signaling, including the PI3K/AKT and MAPK/ERK pathways (12;29). Western blot analysis was used to determine

inhibition of Mer (phospho-Mer) in response to treatment with UNC569 and effects on downstream oncogenic signaling pathways in ALL cells. ALL cells were treated with UNC569 and a dose-dependent decrease in the levels of the active, phosphorylated form of Mer was observed in both 697 B-cell ALL (IC_{50} = 141 ± 15 nM) and Jurkat T-cell ALL (IC_{50} = 193 ± 56 nM) cells (Figures 2A and B). Mer inhibition was achieved with lower UNC569 doses in the 697 cell line compared to the Jurkat cell line (Figure 2A). The Jurkat cell line expressed Mer and Tyro3, but no Axl (Supplementary figure 1). To demonstrate specificity for Mer, we tested whether UNC569 inhibited the activation of Tyro3 (phospho-Tyro3) in addition to Mer. Jurkat cells were treated with UNC569 and no decrease in the levels of the active, phosphorylated form of Tyro3 was detected (Supplementary figure 2), suggesting that any phenotypic effects noted from UNC569 were not mediated via inhibition of the closely related Axl or Tyro3 tyrosine kinases.

Decreased Gas6 ligand-stimulated phosphorylation of ERK was observed in Jurkat cells treated with UNC569 relative to cells treated with vehicle only (Figure 2C). In the 697 cell line, Gas6-stimulated AKT phosphorylation was decreased after treatment with UNC569. We did not anticipate significant changes in AKT activation in the presence of Gas6 or after treatment with UNC569 in Jurkat cells since in these cells AKT is constitutively active due to a mutation in PTEN, a phosphatase that regulates AKT activity (34). These data demonstrate that UNC569 can effectively inhibit the activation of Mer and downstream signaling, including the PI3K/AKT and MAPK/ERK pathways, and indicate a biochemical mechanism by which UNC569 may influence oncogenic processes including cell growth, proliferation and survival of ALL cells.

UNC569 induces apoptosis in ALL cell lines

To determine whether UNC569 inhibits oncogenic phenotypes in ALL cells, 697 and Jurkat cultures were treated with UNC569 or DMSO control only and effects on proliferation and/or survival were examined after 48 hours. Preliminary studies demonstrated efficient Mer inhibition in ALL cells after 24 hours of treatment with UNC569, but phosphorylated Mer levels were increased by 48 hours (Supplementary Figure 3). Thus, for the phenotypic studies described here, UNC569 and medium were replenished after 24 hours in order to ensure continuous Mer inhibition throughout the experiments. First, UNC569 mediated effects on cell number in 697 and Jurkat cultures were determined using the MTT assay. Inhibition of Mer by UNC569 decreased the number of metabolically active Jurkat and 697 cells after 48 hours in culture (Figure 3A). The 697 cell line was more sensitive to UNC569 (IC_{50} = 0.5 μM, 95% confidence interval = 0.35 to 0.75 μM) compared to Jurkat cells (IC_{50} = 1.2 μM, 95% confidence interval = 0.76 to 1.78 μM). This observation was consistent with the relative sensitivity of these cell lines for Mer inhibition by UNC569 (Figure 2A). The results of the MTT assay can be attributed to either a decrease in proliferation or an increase in cell death. To distinguish between these two effects, the incidence of apoptosis in response to treatment with UNC569 was analyzed by flow cytometry after cells were stained with YO-PRO-1 iodide (YoPro) and propidium iodide (PI) dyes to identify early apoptotic (YoPro+) and dead cells (YoPro+, PI+). Both cell lines exhibited a statistically significant increase in the percentage of apoptotic and dead cells in comparison to the DMSO control in response to treatment with UNC569 (Figure 3B). The apoptosis signaling effectors Caspase 3 and PARP were also analyzed. Jurkat and 697 cells treated with UNC569 exhibited increased levels of cleaved Caspase 3 and cleaved PARP compared to cells treated with DMSO control only (Figure 3C), confirming the induction of apoptosis in response to treatment with UNC569.

UNC569 increases sensitivity of leukemia cells to standard ALL chemotherapies

Jurkat and 697 cells were treated with the chemotherapeutic agents methotrexate (MTX) or etoposide (VP 16) for 48 hours, either alone or in combination with UNC569 to investigate the interaction between UNC569 and cytotoxic chemotherapies that are currently in clinical use. Apoptotic and dead cells were detected by flow cytometry after staining with YoPro and PI. Treatment with the low concentration of UNC569 used here was not sufficient to induce significant cell death in the Jurkat and 697 cell lines, but resulted in a significant increase in the percentage of dead cells in response to treatment with methotrexate or etoposide compared to treatment with the chemotherapeutic agents alone (Figure 4A and B). More specifically, treatment with UNC569 resulted in a significant increase in apoptotic and dead cells in Jurkat cultures treated with methotrexate relative to cultures treated with methotrexate alone (26.4 ± 2.9 % versus 17.5 ± 1.3 %, $p = 0.03$). Similarly, treatment of 697 cells with UNC569 resulted in a statistically significant increase in apoptotic and dead cells compared with etoposide alone (43.3 ± 2.6 % versus 33.03 ± 0.42 %, $p = 0.02$) and a trend when compared methotrexate alone (28.93 ± 4.96 % versus 18.13 ± 3.63 %, $p = 0.1$). These results demonstrate increased sensitivity of ALL cells to cytotoxic chemotherapies in response to Mer inhibition with UNC569.

UNC569 decreases colony formation in ALL cell lines

To further investigate whether Mer inhibition by UNC569 resulted in changes in the oncogenic properties of ALL cells, colony forming potential in methylcellulose-based medium was assessed. Treatment with UNC569 (400 nM) significantly inhibited the ability of the 697 (Figure 5A, 95.9 ± 16.8 versus 14.8 ± 12.8 colonies, $p = 0.02$) and Jurkat (Figure 5B, 100.1 ± 23.4 versus 25.6 ± 6.4 colonies, $p = 0.04$) cell lines to form colonies compared to cells treated with DMSO control only. Both the size (Figure 5C) and the number (Figure 5D) of the colonies were decreased with increasing doses of UNC569. In contrast, Jurkat cells treated with the control compound UNC1653 did not show any reduction of colony formation in methylcellulose (Supplementary Figure 4). UNC1653 is a structurally to UNC569 related negative control compound, which does not inhibit Mer (data not shown).

UNC569 inhibits Mer phosphorylation, reduces proliferation and/or survival and reduces colony formation in BT12 pediatric rhabdoid tumor cells

We repeated similar analysis in the BT12 adherent atypical teratoid rhabdoid tumor cell line with the aim to test whether UNC569 had anti-oncogenic effects in a pediatric solid tumor. Western blot analysis was used to determine inhibition of phospho-Mer in response to treatment with UNC569 in atypical teratoid rhabdoid tumor cells. BT12 cells were treated with UNC569 and a dose-dependent inhibition Mer phosphorylation was observed (Figure 6A). To investigate whether UNC569 inhibits oncogenic phenotypes in BT12 cells, proliferation and/or survival were examined using a MTT assay after 48 hours of treatment with UNC569 or vehicle only. Inhibition of Mer by UNC569 significantly decreased the number of metabolically active BT12 cells after 48 hours in culture (Figure 6B, $IC_{50} = 0.85$ μM, 95% confidence interval = 0.4 to 1.7 μM). UNC569 inhibited colony formation of 697 and Jurkat cells in methycellulose. Further colony forming potential in soft agar was assessed to examine whether Mer inhibition by UNC569 resulted in changes in the oncogenic properties of BT12 cells. Treatment with UNC569 (1 μM) significantly inhibited the ability of the BT12 cell line (294.7 ± 16.6 versus 175.1 ± 28.3 colonies, $p = 0.02$) to form colonies compared to cells treated with vehicle only (Figure 6C and D).

UNC569 induces disease regression in a transgenic zebrafish model

The effect of UNC569 in an *in vivo* model of T-ALL was examined using a transgenic zebrafish expressing lymphocyte-specific human MYC controlled by the native zebrafish

rag2 promoter (Figure 7A). These fish develop highly-penetrant T-cell malignancies (31). This line was bred to a second transgenic zebrafish line with T-cell specific enhanced green fluorescent protein (GFP) expression (32). Consequently, T-cell cancers in these animals are GFP positive (GFP^+). Leukemic zebrafish were treated continuously for 2 weeks by immersion in 4 μM UNC569, DMSO alone, or mock-treated in water only. Images were captured before and after treatment with UNC569, and GFP fluorescence intensity was determined as an indicator of tumor burden. UNC569-treated animals showed ≥ 50 % disease regression in 10/18 fish, compared to > 50 % responses in only 2/14 DMSO-treated and 0/10 mock-treated animals, respectively (Figure 7 and Supplementary Figure 5). Tumor burden decreased by an average of 47.8 % (Figure 7B), with only 2/18 animals having progression during treatment. DMSO-treated fish typically had either progressive (6/14 fish) or stable (≤ 20 % regression; 4/14 fish) disease, leading to an average tumor increase of 13.0 %. Likewise, mock-treated fish exhibited an average increase in tumor burden of 9.9 % (Figure 7B), with 4/10 animals having outright progression and 5/10 having stable disease. The 47.8 % reduction in tumor burden in UNC569-treated animals was statistically superior to the 13.0 % and 9.9 % increases observed in the two control groups ($p = 0.0013$ and 0.0003, respectively). Even in short treatment courses against already-established cancers, UNC569 clearly demonstrates potent *in vivo* efficacy as a single agent against T-ALL, with no apparent toxicity.

Discussion

Mer contributes to leukemogenesis and progression of B- and T-cell ALL (10;11). In this study, we have extended our previous finding of ectopic Mer expression in human ALL and evaluated Mer inhibition as a novel therapeutic strategy for treatment of ALL. In addition, as a critical step toward development of translational agents targeting Mer for oncology applications, we investigated the utility of a novel, first in class Mer selective small molecule tyrosine kinase inhibitor, UNC569, for treatment of ALL using cell culture and zebrafish models.

The studies described here demonstrate potent inhibition of Mer by UNC569 in both B-ALL and T-ALL cell lines. Previous studies have demonstrated activation of MAPK/ERK and PI3K/AKT signaling pathways downstream of Mer in tumor cells and roles for these proteins in cell survival and proliferation are well established (12;29;35;36). Consistent with these observations, we found activation of these pathways downstream of Gas6 in the 697 and Jurkat ALL cell lines. Furthermore, treatment with UNC569 resulted in decreased activation of downstream signaling molecules, including phospho-ERK and phospho-AKT (Figure 2C). UNC569-mediated inhibition of Mer-dependent pro-survival pathways resulted in dose-dependent induction of apoptosis (Figure 3B and C) and decreased colony forming potential in methylcellulose (Figure 5). Thus, UNC569 inhibits oncogenic signaling and oncogenic properties in leukemia cells. In addition, inhibition of Mer with UNC569 resulted in increased cell death in response to treatment with methotrexate and etoposide (Figure 4A and B). These data suggest that Mer inhibition may be particularly effective in combination with cytotoxic chemotherapies, allowing for increased therapeutic response and/or reduction of chemotherapy dose and associated potential side effects. Of note, methotrexate is used in standard pediatric ALL chemotherapy regimens and etoposide is a major component of relapse therapy. Similar results were recently reported for the 697 and Jurkat shRNA Mer knockdown (12;36). A shRNA Mer knockdown led to decreased ERK/AKT activation, increased apoptosis, a chemosensitization with commonly used chemotherapeutic agents, and a decreased colony forming potential in methylcellulose or soft agar. Thus, these data provide rationale for introduction of Mer TKIs into the clinic in combination with agents that are already known to be clinically effective.

In addition, in an effort to expand upon potential clinical utilities of UNC569, we investigated the potential efficacy of this ligand for the treatment of ATRT. Despite some development in the treatment of ATRT (37;38), long-term outcomes remain not optimal. Further, current multimodality therapy regimes for ATRT are toxic and associated with short- and long-term toxicities. ATRT is a malignancy that requires the development of more effective and less toxic therapies to improve survival. We have demonstrated in this study that the treatment of the ATRT cell line BT12 with UNC569 resulted in an inhibition of Mer activation (Figure 6A), in a decrease of metabolically active cells measured by MTT (Figure 6B) and in a reduction of the ability of colony formation in soft agar (Figure 6C and D).

Lastly, UNC569 showed potent efficacy as a single agent in a zebrafish model of MYC-driven T-ALL, with many animals showing significant regression of established tumors after only two weeks of treatment (Figure 7 and Supplementary Figure 5). Notably, toxicity was not observed in these *in vivo* assays. Taken together these results suggest that Mer inhibition may have utility as a single-agent and may also synergize with standard chemotherapeutics to enhance cancer cell death in both solid tumors and hematopoietic malignancies.

Supplementary Material

Refer to Web version on PubMed Central for supplementary material.

Acknowledgments

In vivo imaging was performed using the IVIS Shared Resource at the University of Colorado Cancer Center (supported by grant P30-CA046934). *In vitro* imaging experiments were performed at the University of Colorado Anschutz Medical Campus Advance Light Microscopy Core supported in parts by NIH/NCRR Colorado CTSI Grant Number UL1 RR025780. The authors wish to thank Karen Helm, Christine Childs, and Lester Acosta at the University of Colorado Cancer Center Flow Cytometry Core for their expert technical assistance (supported by grant P30CA046934) and Randall Wong of the University of Colorado Denver Diabetes & Endocrinology Research Center Molecular Biology Core Facility (supported by NIH P30 DK57516) for cell line authentication services.

Funding

This work was supported in parts by the National Institute of Health (RO1CA137078 to D.K. Graham) and by a CureSearch Research Fellowship Award (#020660 to J.K. Frazer). D.K. Graham is a Damon Runyon-Novartis Clinical Investigator supported in parts by the Damon Runyon Cancer Research Foundation (CI-39-07). Funding was also provided by the National Cancer Institute, National Institute of Health, under Contract No. HHSN261200800001E. The content of this publication does not necessarily reflect the views or policies of the Department of Health and Human Services, nor does mention of trade names, commercial products, or organizations imply endorsement by the U.S. Government.

Reference List

1. Kaatsch P. Epidemiology of childhood cancer. Cancer Treat Rev. 2010; 36:277–285. [PubMed: 20231056]
2. Jemal A, Siegel R, Xu J, Ward E. Cancer Statistics 2010. CA Cancer J Clin. 2010; 60:277–300. [PubMed: 20610543]
3. Pui C, Mullighan C, Evans W, Relling M. Pediatric acute lymphoblastic leukemia: where are we going and how do we get there? Blood. 2012; 120:1165–1174. [PubMed: 22730540]
4. Landier W, Bhatia S. Cancer survivorship: a pediatric perspective. Oncologist. 2008; 13:1181–1192. [PubMed: 18987046]
5. Oeffinger K, Mertens A, Sklar C, Kawashima T, Hudson M, Meadows A, et al. Chronic health conditions in adult survivors of childhood cancer. N Engl J Med. 2006; 355:1572–1582. [PubMed: 17035650]

6. Linger R, Keating A, Earp H, Graham D. TAM receptor tyrosine kinases: biologic functions, signaling, and potential therapeutic targeting in human cancer. Adv Cancer Res. 2008; 100:35–83. [PubMed: 18620092]
7. Brandao L, Migdall-Wilson J, Eisenman K, Graham D. TAM Receptors in Leukemia: Expression, Signaling, and Therapeutic Implications. Crit Rev Oncog. 2011; 16:47–63. [PubMed: 22150307]
8. Linger R, Keating A, Earp H, Graham D. Taking aim at Mer and Axl receptor tyrosine kinases as novel therapeutic targets in solid tumors. Expert Opin Ther Targets. 2010; 14:1073–1090. [PubMed: 20809868]
9. Yeoh E, Ross M, Shurtleff S, Williams W, Patel D, Mahfouz R, et al. Classification, subtype discovery, and prediction of outcome in pediatric acute lymphoblastic leukemia by gene expression profiling. Cancer Cell. 2002; 1:133–143. [PubMed: 12086872]
10. Keating A, Salzberg D, Sather S, Liang X, Nickoloff S, Anwar A, et al. Lymphoblastic leukemia/lymphoma in mice overexpressing the Mer (MerTK) receptor tyrosine kinase. Oncogene. 2006; 25:6092–6100. [PubMed: 16652142]
11. Graham D, Salzberg D, Kurtzberg J, Sather S, Matsushima G, Keating A, et al. Ectopic expression of the proto-oncogene Mer in pediatric T-cell acute lymphoblastic leukemia. Clin Cancer Res. 2006; 12:2662–2669. [PubMed: 16675557]
12. Brandao L, Winges A, Christoph S, Sather S, Migdall-Wilson J, Schlegel J, et al. Inhibition of MerTK increases the chemosensitivity and decreases the oncogenic potential in T-cell acute lymphoblastic leukemia. Blood Cancer Journal. 2013; 3:e101. [PubMed: 23353780]
13. Cummings C, Deryckere D, Earp H, Graham D. Molecular Pathways: MERTK Signaling in Cancer. Clin Cancer Res. 2013 Epub ahead of print.
14. Levy J, Thorburn A. Modulation of pediatric brain tumor autophagy and chemosensitivity. J Neurooncol. 2012; 106:281–290. [PubMed: 21842312]
15. Ginn K, Gajjar A. Atypical teratoid rhabdoid tumor: current therapy and future directions. Front Oncol. 2012; 2:114. [PubMed: 22988546]
16. O'Brien S, Guilhot F, Larson R, Gathmann I, Baccarani M, Cervantes F, et al. Imatinib compared with interferon and low-dose cytarabine for newly diagnosed chronic-phase chronic myeloid leukemia. N Engl J Med. 2003; 348:994–1004. [PubMed: 12637609]
17. O'Hare T, Deininger M, Eide C, Clackson T, Druker B. Targeting the BCR-ABL signaling pathway in therapy-resistant Philadelphia chromosome-positive leukemia. Clin Cancer Res. 2011; 17:212–221. [PubMed: 21098337]
18. Goldman J. Ponatinib for chronic myeloid leukemia. N Engl J Med. 2012; 367:2148–2149. [PubMed: 23190226]
19. Brassard M, Rondeau G. Role of vandetanib in the management of medullary thyroid cancer. Biologics. 2012; 6:59–66. [PubMed: 22500115]
20. Ryan Q, Ibrahim A, Cohen M, Johnson J, Ko C, Sridhara R, et al. FDA drug approval summary: lapatinib in combination with capecitabine for previously treated metastatic breast cancer that overexpresses HER-2. Oncologist. 2008; 13:1114–1119. [PubMed: 18849320]
21. Wang Y, Schmid-Bindert G, Zhou C. Erlotinib in the treatment of advanced non-small cell lung cancer: an update for clinicians. Ther Adv Med Oncol. 2012; 4:19–29. [PubMed: 22229045]
22. Wood L. Sunitinib malate for the treatment of renal cell carcinoma. Expert Opin Pharmacother. 2012; 13:1323–1336. [PubMed: 22607009]
23. Zauli G, Voltan R, Tisato V, Secchiero P. State of the art of the therapeutic perspective of sorafenib against hematological malignancies. Curr Med Chem. 2012; 19:4875–4884. [PubMed: 22934770]
24. Chapman P, Hauschild A, Robert C, Haanen J, Ascierto P, Larkin J, et al. Improved survival with vemurafenib in melanoma with BRAF V600E mutation. N Engl J Med. 2011; 364:2507–2516. [PubMed: 21639808]
25. Huang X, Finerty PJ, Walker J, Butler-Cole C, Vedadi M, Schapira M, et al. Structural insights into the inhibited states of the Mer receptor tyrosine kinase. J Struct Biol. 2009; 165:88–96. [PubMed: 19028587]
26. Verma A, Warner S, Vankayalapati H, Bearss D, Sharma S. Targeting Axl and Mer kinases in cancer. Mol Cancer Ther. 2011; 10:1763–1773. [PubMed: 21933973]

27. Liu J, Yang C, Simpson C, Deryckere D, Van Deusen A, Miley M, et al. Discovery of Novel Small Molecule Mer Kinase Inhibitors for the Treatment of Pediatric Acute Lymphoblastic Leukemia. ACS Med Chem Lett. 2012; 3:129–134. [PubMed: 22662287]
28. Masters J, Thomson J, Daly-Burns B, Reid Y, Dirks W, Packer P, et al. Short tandem repeat profiling provides an international reference standard for human cell lines. Proc Natl Acad Sci U S A. 2001; 98:8012–8017. [PubMed: 11416159]
29. Linger R, Cohen R, Cummings C, Sather S, Migdall-Wilson J, Middleton D, et al. Mer or Axl receptor tyrosine kinase inhibition promotes apoptosis, blocks growth and enhances chemosensitivity of human non-small cell lung cancer. Oncogene. 2013; 32:3420–3431. [PubMed: 22890323]
30. Mahajan N, Earp H. An SH2 domain-dependent, phosphotyrosine-independent interaction between Vav1 and the Mer receptor tyrosine kinase: a mechanism for localizing guanine nucleotide-exchange factor action. J Biol Chem. 2003; 278:42596–42603. [PubMed: 12920122]
31. Gutierrez A, Grebliunaite R, Feng H, Kozakewich E, Zhu S, Guo F, et al. Pten mediates Myc oncogene dependence in a conditional zebrafish model of T cell acute lymphoblastic leukemia. J Exp Med. 2011; 208:1595–1603. [PubMed: 21727187]
32. Langenau D, Ferrando A, Traver D, Kutok J, Hezel J, Kanki J, et al. In vivo tracking of T cell development, ablation, and engraftment in transgenic zebrafish. Proc Natl Acad Sci U S A. 2004; 101:7369–7374. [PubMed: 15123839]
33. Ridges S, Heaton W, Joshi D, Choi H, Eiring A, Batchelor L, et al. Zebrafish screen identifies novel compound with selective toxicity against leukemia. Blood. 2012; 119:5621–5631. [PubMed: 22490804]
34. Shan X, Czar M, Bunnell S, Liu P, Liu Y, Schwartzberg P, et al. Deficiency of PTEN in Jurkat T cells causes constitutive localization of Itk to the plasma membrane and hyperresponsiveness to CD3 stimulation. Mol Cell Biol. 2000; 20:6945–6857. [PubMed: 10958690]
35. Keating A, Kim G, Jones A, Donson A, Ware K, Mulcahy J, et al. Inhibition of Mer and Axl receptor tyrosine kinases in astrocytoma leads to increased apoptosis and improved chemosensitivity. Mol Cancer Ther. 2010; 9:1298–1307. [PubMed: 20423999]
36. Linger R, Lee-Sherick A, Deryckere D, Cohen R, Jacobsen K, McGranahan A, et al. Mer receptor tyrosine kinase is a therapeutic target in pediatric B-cell acute lymphoblastic leukemia. Blood. 2013 Epub ahead of print.
37. Gardner S, Asgharzadeh S, Green A, Horn B, McCowage G, Finlay J. Intensive induction chemotherapy followed by high dose chemotherapy with autologous hematopoietic progenitor cell rescue in young children newly diagnosed with central nervous system atypical teratoid rhabdoid tumors. Pediatr Blood Cancer. 2008; 51:235–240. [PubMed: 18381756]
38. Knipstein J, Birks D, Donson A, Alimova I, Foreman N, Vibhakar R. Histone deacetylase inhibition decreases proliferation and potentiates the effect of ionizing radiation in atypical teratoid/rhabdoid tumor cells. Neuro Oncol. 2012; 14:175–183. [PubMed: 22156471]

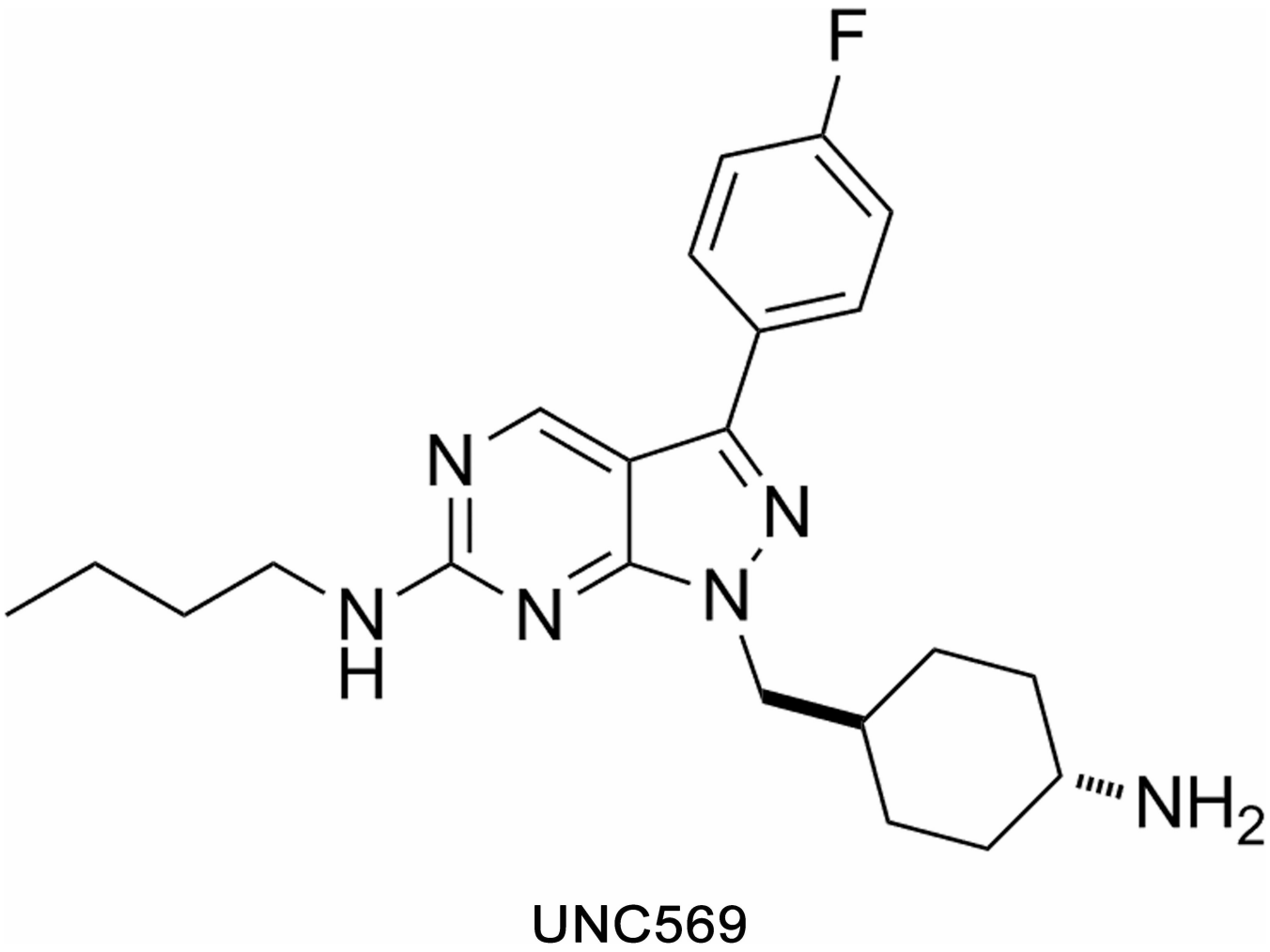

Figure 1. Chemical structure of UNC569

Chemical structure of the Mer tyrosine kinase inhibitor UNC569 based on the pyrazolopyrimidine scaffold.

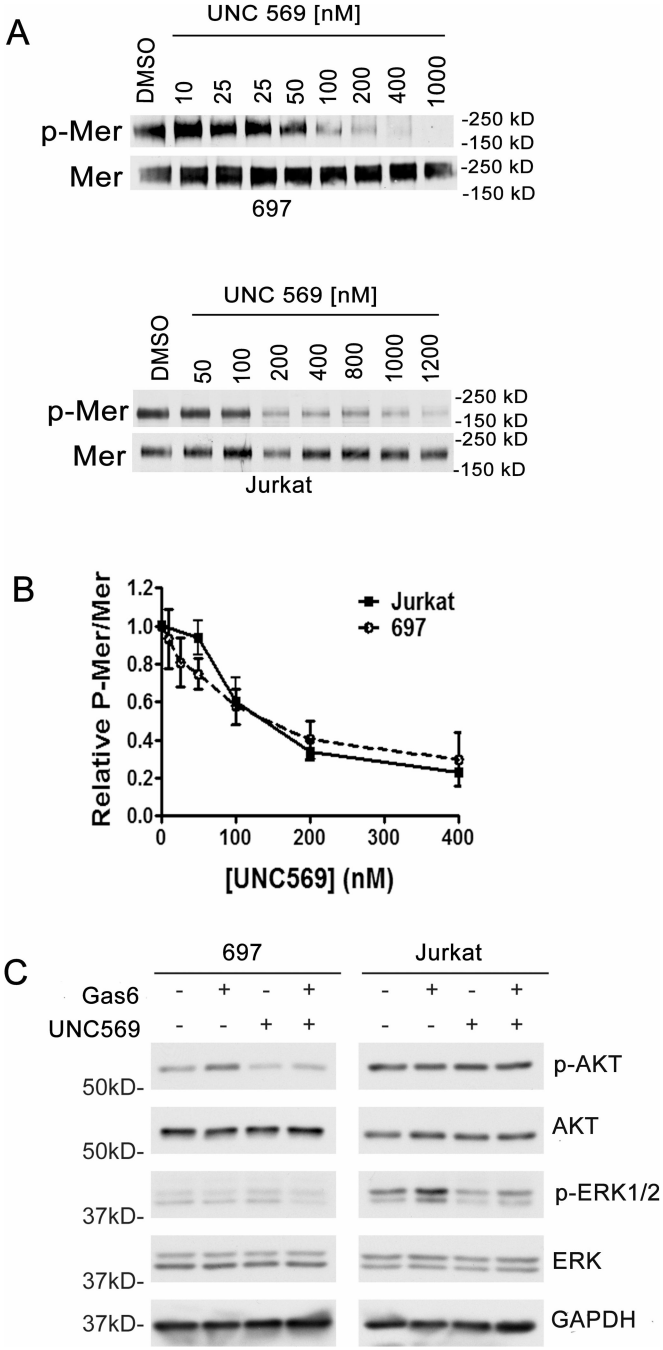

Figure 2. UNC569 inhibits Mer phosphorylation and downstream signalling in acute lymphoblastic leukemia cells

(A) Jurkat and 697 cell cultures were treated with the indicated concentrations of UNC569 for 1 hour. Pervanadate was added to cell cultures for 3 minutes to stabilize the phosphorylated form of Mer. Mer was immunoprecipitated from cell lysates and Mer phospho-protein (p-Mer) and Mer total-protein (Mer) were detected by western blot. (B) Relative levels of p-Mer and Mer proteins were determined. Mean values +/− standard error derived from 4 independent experiments are shown. (C) Jurkat and 697 cell cultures were incubated in serum-free medium for two hours followed by additional 90-minutes in the presence of UNC569 (1 μM) or DMSO control. Cells were then stimulated with (+) or

without (−) 200 nM rhGas6 and phosphorylated AKT (p-AKT), AKT, phosphorylated ERK1/2 (p-ERK), and ERK1/2 proteins were detected in whole-cell lysates by western blot analysis. GAPDH protein was detected as a loading control. Numbers on the left indicate the location of molecular weight (kD) markers. Immunoblots are representative of at least three independent experiments.

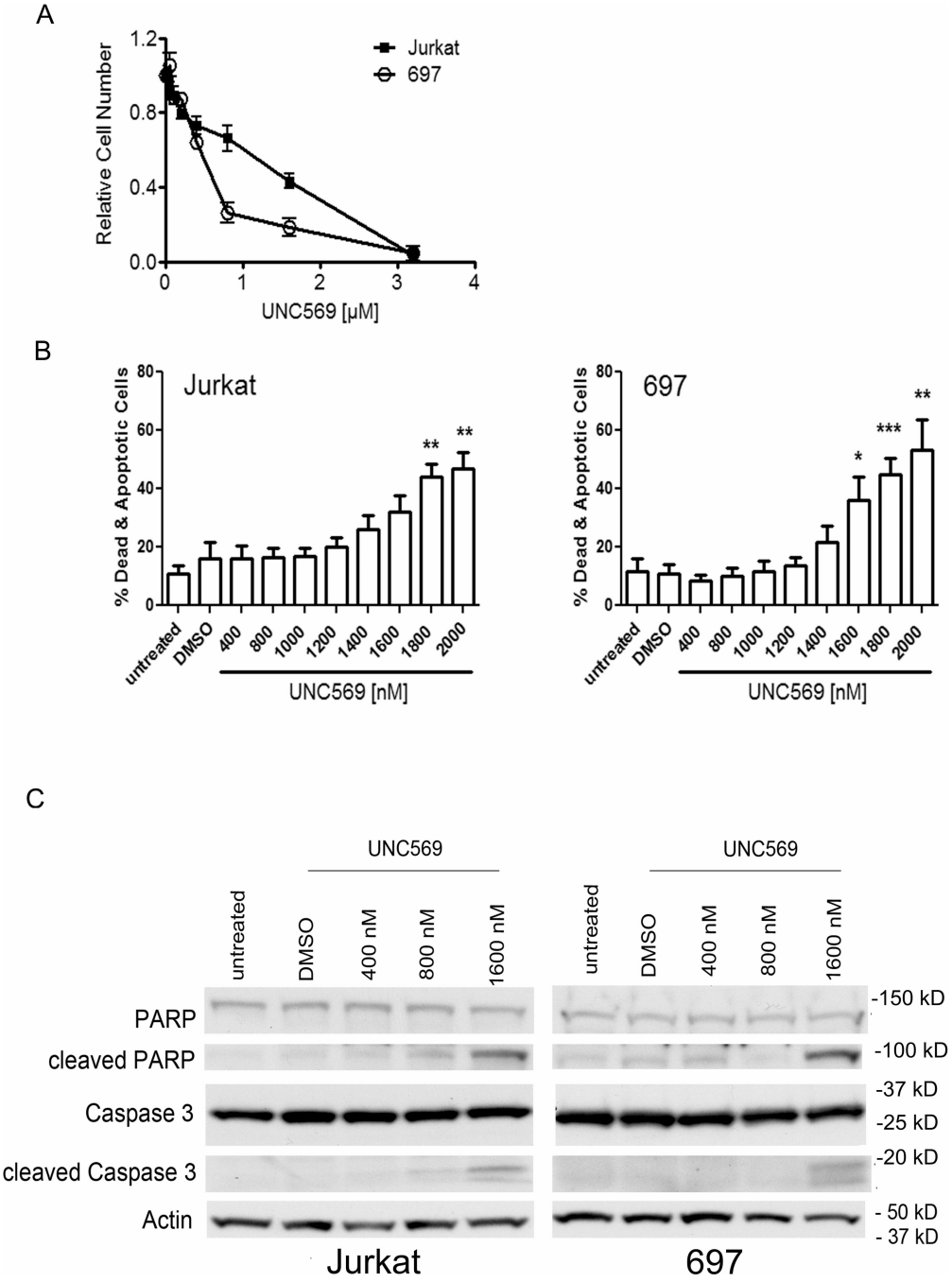

Figure 3. UNC569 reduces proliferation and/or survival and induces apoptosis in ALL cells

Cells were cultured at optimal density (3×10^5/ml) such that nutrients would not be limiting and treated with the indicated concentrations of UNC569. After 24 hours, cells were harvested and cultured in fresh medium containing the indicated concentrations of UNC569 for an additional 24 hours. (A) Relative numbers of metabolically active cells were determined by MTT assay. Mean values and standard errors derived from 3 independent experiments are shown. (B) Cells were stained with YO-PRO-1 iodide (YoPro) and propidium iodide (PI). Apoptotic (YoPro+) and dead (YoPro+, PI+) cells were identified by flow cytometry. Mean values +/− standard errors derived from 3 independent experiments are shown. (C) Whole-cell lysates were prepared and the indicated proteins were detected by

western blot. Actin was detected as a loading control. Western blots are representative of 3 independent experiments.

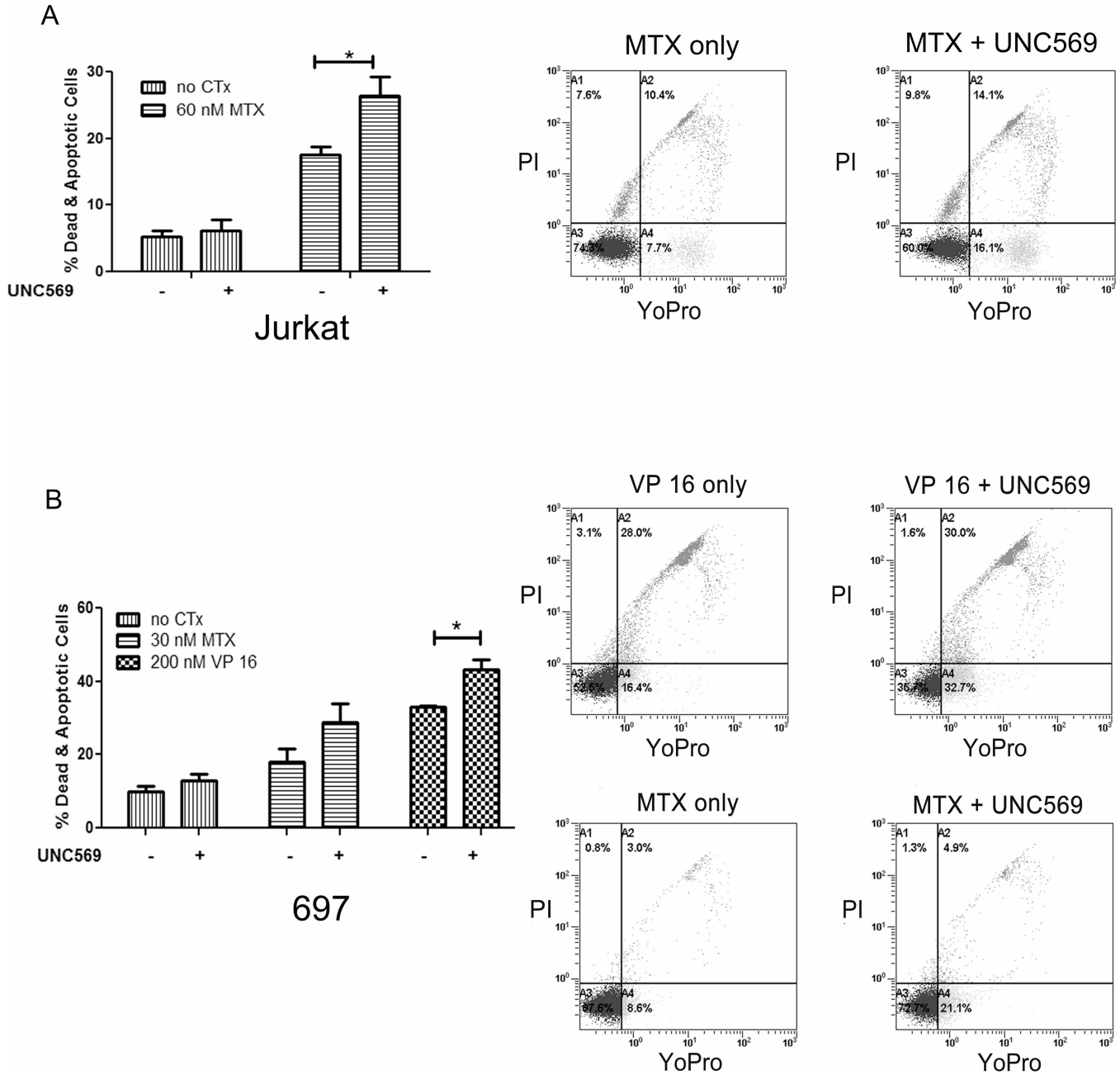

Figure 4. Treatment with UNC569 results in an increase in chemosensitivity of ALL cells

Jurkat (A) or 697 (B) cells were exposed to etoposide (VP 16) and/or methotrexate (MTX) alone and in combination with UNC569 (500 nM) for 48 hours. Apoptotic and dead cells were identified by flow cytometric analysis of cells stained with YO-PRO-1 iodide and propidium iodide. Representative flow cytometric profiles are shown. Mean values +/− standard errors are derived from at least 3 independent experiments.

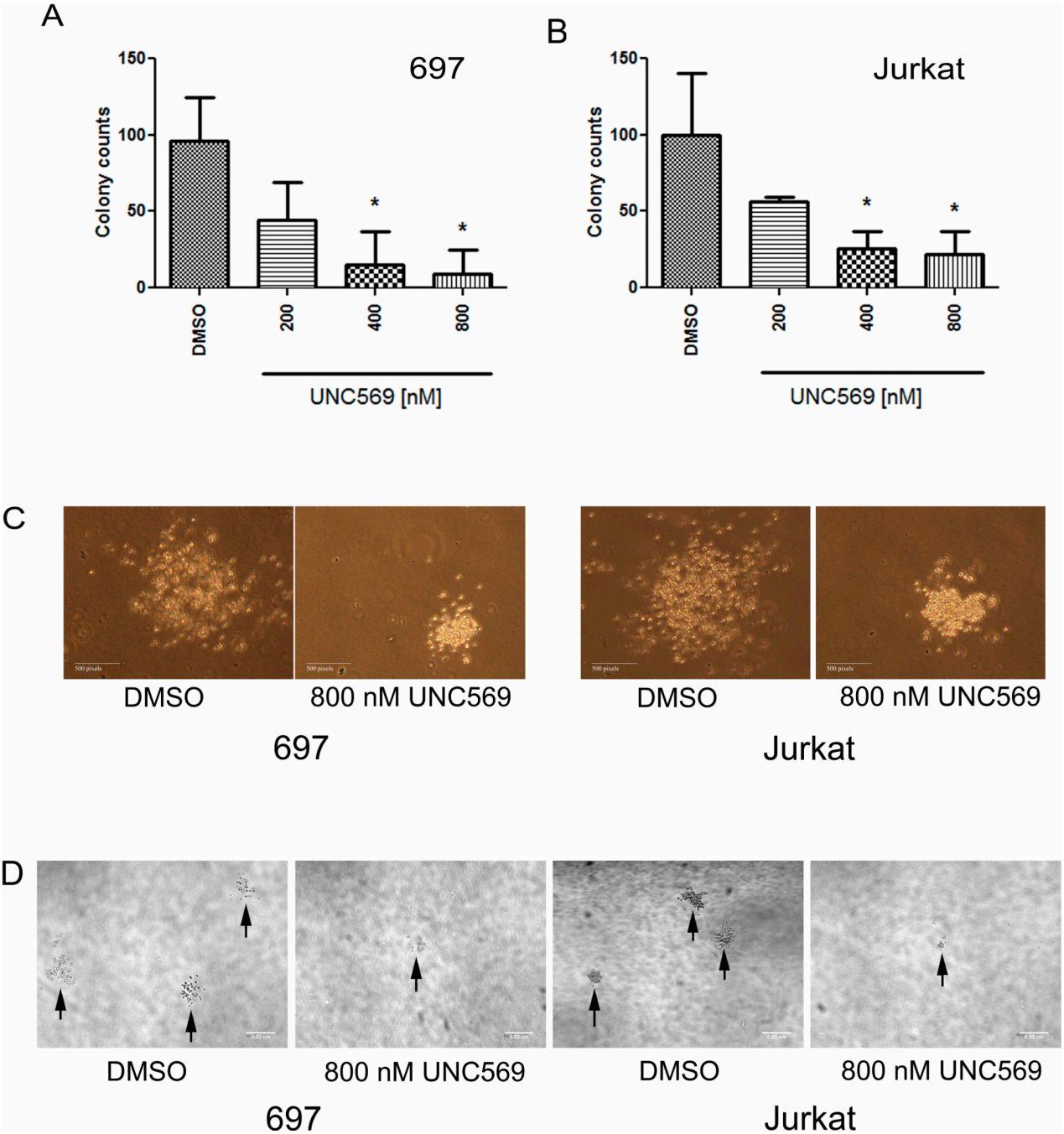

Figure 5. UNC569 reduces colony formation in Jurkat and 697 cell lines

Cells were plated in methylcellulose in the presence of the indicated concentrations of UNC569 or DMSO control only. Every 48 hours, fresh culture medium containing UNC569 or DMSO was added. Colonies were counted after eight days. Long-term colony growth of 697 (A) and Jurkat (B) cells in methylcellulose is shown. Mean values +/− standard errors were derived from 3 independent experiments. (C) Representative colonies from the Jurkat and 697 cell lines after treatment with the indicated concentrations of UNC569 or DMSO control only. Single colony pictures were generated using a Nikon Eclipse TS100 microscope with Nikon Plan 10X, numerical aperture 0.25 objective lens and with a Nikon Digital Sight DS-L2 camera equipped with Firmware DS-L2 Ver4.60. (D) Representative

fields from methylcellulose cultures of the Jurkat and 697 cell lines after treatment with UNC569 or DMSO control only. Bright field images were taken with a spinning disk confocal 3I Marianas based on a inverted Zeiss Axio Observer Z1. A CoolSnap HQ2 camera featuring 1392 × 1040 imaging pixels via a 5× Zeiss air objective was used. As imaging acquisition software Slidebook 5.0 was utilized.

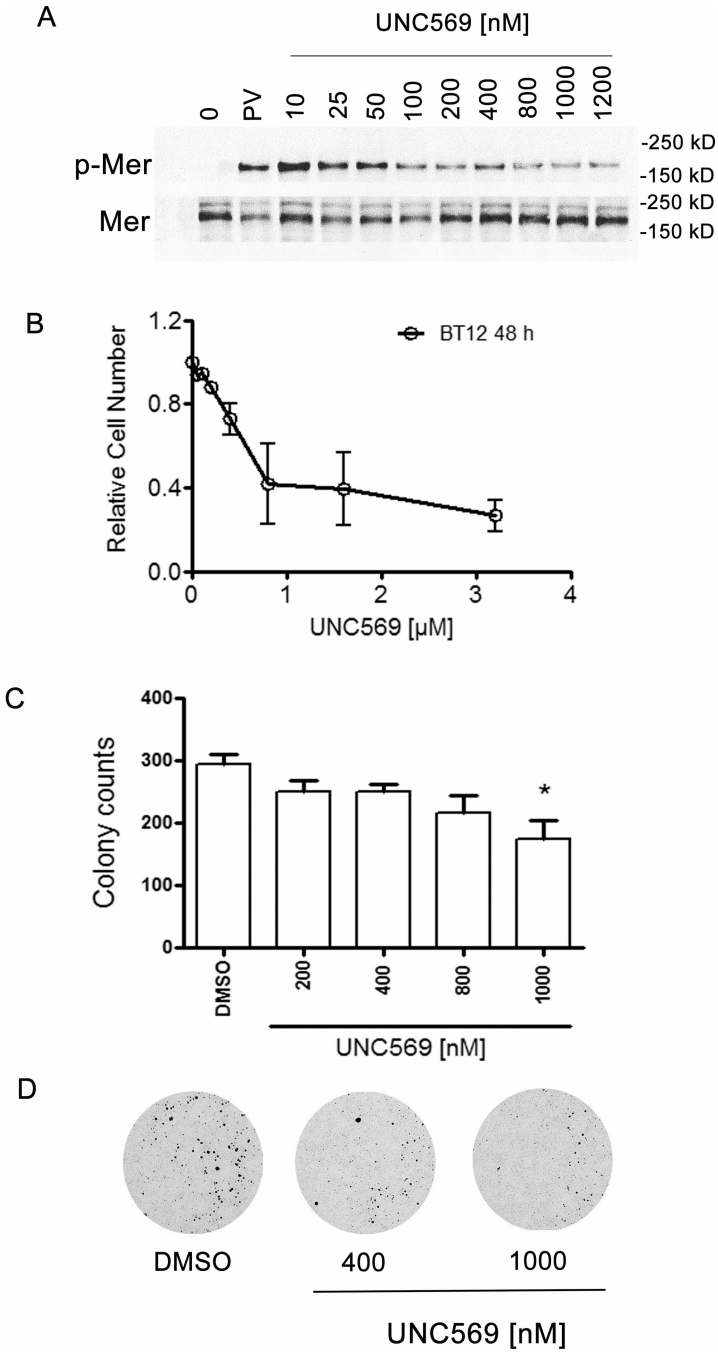

Figure 6. UNC569 inhibits Mer phosphorylation, reduces proliferation and/or survival and reduces colony formation in BT12 pediatric rhabdoid tumor cells

(A) Phosphorylated Mer (p-Mer) and Mer levels were evaluated by western blot following treatment with UNC569. BT12 cell cultures were treated with the indicated concentrations of UNC569. Pervanadate was added to cultures for 3 minutes to stabilize the phosphorylated form of Mer. Cells were lysed, immunoprecipitated with polyclonal C-terminal Mer antibody N-14 and subjected to SDS-polyacrylamide gel electrophoresis. Gels with electrophoresed, Mer immunoprecipitates were transferred and blotted with phosphotyrosine antibody or back blotted with the NIH anti-Mer polyclonal. (B) UNC569 reduces proliferation and/or survival of BT12 cells. These data were obtained using the MTT assay.

Cell cultures were treated with the indicated concentrations of UNC569 for 48 hours and relative cell numbers were determined. Mean values +/− standard errors derived from 3 independent experiments are shown. (C) UNC569 reduces long-term colony growth of BT12 cells in soft agar assay. Cells were plated in soft agar in the presence of the indicated concentrations of UNC569. Mean values +/− standard errors derived from 3 independent experiments are shown. (D) Representative pictures from BT12 soft agar cultures treated with the indicated concentrations of UNC569 or DMSO control only. Pictures are scans made with Perfection V700 Scanner.

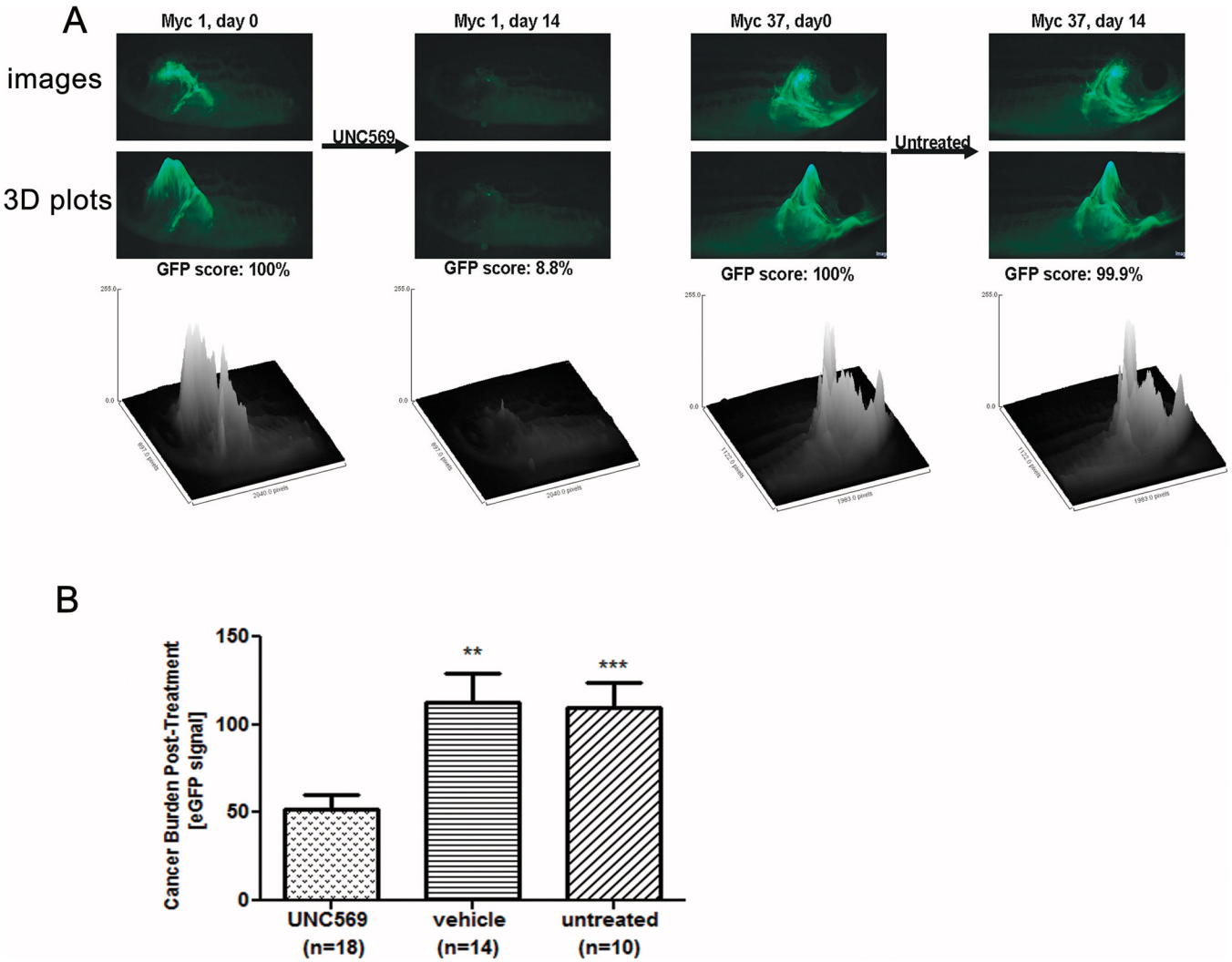

Figure 7. UNC569 induces disease regression in a transgenic zebrafish model

Zebrafish with GFP^{+} T-lymphoblastic cancers caused by transgenic human MYC were treated with 4 μM UNC569, DMSO control, or mock-treated for 2 weeks. (A) Images at top show the same fish (Myc1) before (left) and after (right) 4 μM UNC569 treatment × 14 days. To quantify tumor burden, GFP intensity was reconfigured as a 3 dimensional plot (images and graph below) and integrated for volume. Pre-treatment plots were assigned GFP scores = 100 %; post- (day 14) treatment scores reflect % of original GFP intensity remaining (i.e., Myc1 post GFP score = 8.8 %, or 91.2 % regression). Myc37 images show a mock-treated fish with stable disease (pre GFP score = 100 %, post = 99.9 %). (B) UNC569-treated fish (n = 18) had average regressions of 47.8 %. Vehicle (n = 14) and mock (n = 10) treatments had statistically significant progressions of 13.0 % and 9.9 % (UNC569 vs. DMSO, p = 0.0013**; UNC569 vs. mock, p = 0.0003***).